Mechanisms of Ion Ejection from Liquid Beam under Irradiation of Laser by Simultaneous Detection of Ions Produced inside a Liquid Beam and Ejected into a Vacuum

Jun-ya Kohno, Fumitaka Mafuné, and Tamotsu Kondow*

East Tokyo Laboratory, Genesis Research Institute, Inc., and Cluster Research Laboratory, Toyota Technological Institute, 717−86 Futamata, Ichikawa, Chiba 272−0001, Japan

Received: July 13, 1999; In Final Form: October 25, 1999

An aniline solution in 1-propanol, or a pure ethanol liquid, was introduced into vacuum as a continuous liquid flow (liquid beam) and was irradiated with a 266-nm laser. Ions were produced in the liquid beam by multiphoton absorption and partially ejected into the vacuum. The abundance of ions remaining inside the liquid beam and that ejected in the gas phase were measured simultaneously by using an inductive detector and a time-of-flight mass spectrometer, respectively, as a function of irradiation-laser power. The result is explained by the Coulomb ejection model for the ion ejection from the liquid surface. The essential feature changes slightly with the rate of the ion diffusion with respect to that of the ion ejection.

Introduction

A liquid beam technique has been recognized as a powerful tool for advancing our understanding of the structure and dynamics of molecules on a solution surface, since a continuous liquid flow (liquid beam) is proved to be stable even inside the vacuum and enables us to characterize molecules, ions, and electrons ejected from the liquid surface.[1−12] Faubel et al. have measured the kinetic energies of molecules evaporating from a liquid beam of aqueous solution and elucidated that water molecules on the liquid beam surface are supercooled.[3,4] Brutschy et al. have employed a liquid beam as an interface between a liquid chromatograph and a mass spectrometer and observed ions of nonvolatile species such as protein in the gas phase.[13,14]

In our previous studies, we have reported a technique of preparing a liquid beam in a vacuum and observed the cluster ions ejected from the liquid surface following resonant multiphoton ionization by a time-of-flight (TOF) mass spectrometer.[1,2] Taking this technique, we have investigated solvation structures and reactions occurring in the vicinity of a liquid beam surface by observing cluster ions ejected from it:[7−11] When molecules in the liquid beam are ionized by irradiation of the laser, electrons are liberated selectively from a surface region, so that the surface is charged up positively.[15] The electrons tend to be captured in the liquid beam as solvated electrons, negative ions, and/or a geminate recombination, and as a result, a number density of the positive charges (electron depletion) decreases exponentially with the depth from the surface.[16] As the laser power increases, the density of the positive charges increases and exceeds a threshold value, above which an ion is ejected into vacuum by Coulomb repulsion force exerted by the positive charges.[17] The dependence of the ion intensity on the laser power[17] and the shape of the TOF mass peaks[7] are explained well by this scheme (Coulomb ejection model).[18]

According to this model, photoions are expected to be generated inside the liquid beam even below the threshold laser power, below which no ion is observed in the gas phase. Even above the threshold laser power, a part of the photoions remains inside the liquid beam. Therefore, the validity of this model can be examined by simultaneous detection of the ions in the liquid beam and those ejected into vacuum. To detect ions produced in the liquid, we developed an inductive detector for the measurement of ion abundance inside the liquid beam. An electric current induced by ions in a liquid beam flowing through the detector is measured as a function of time. The induction charge obtained by integrating the induction current is proportional to the number of ions in the liquid beam.

The purpose of the present study is to elucidate the ionization and the ion ejection mechanism in detail by use of an 0.2 M aniline−propanol (PrOH) solution and pure liquid ethanol. Ions ejected from the liquid beam and those remaining inside the liquid beam following photoionization were simultaneously observed by means of a TOF mass spectrometer and the inductive detector as a function of the laser power. The result is explained in principle by the Coulomb ejection model.

Experimental Section

Figure 1 shows a schematic diagram of the liquid beam source, the inductive detector, and the time-of-flight mass spectrometer with a reflectron used in the present study. A 0.2 M aniline solution in 1-propanol or pure ethanol was pressurized by a Shimadzu LC-6A pump designed for a liquid chromatograph and introduced into a vacuum chamber through an aperture with a diameter of 20 μm as a continuous liquid flow (liquid beam). The flow rate (0.2−0.6 mL/min) was kept constant by the pump and a conventional damper. The liquid beam behaves as if it were a stable liquid filament and provides an optical diffraction pattern due to laser illumination perpendicular to the liquid beam. The diameter of the liquid beam was estimated to be 20 μm by analyzing the optical diffraction pattern at 266 nm; the diameter is same as that of the pinhole of the nozzle (ca. 20 μm). The surface of the liquid beam was also examined by monitoring the diffraction pattern at different distances from the nozzle exit along the liquid beam axis: The surface was flat within several millimeters downstream from the nozzle and tended to be distorted apart from the distance.[19]

Traveling a distance of 10 cm from the nozzle, the liquid beam was trapped by a cryopump cooled by liquid nitrogen.

* Corresponding author. E-mail: kondow@utsc.s.u-tokyo.ac.jp

10.1021/jp992364n CCC: $19.00 © 2000 American Chemical Society
Published on Web 12/16/1999

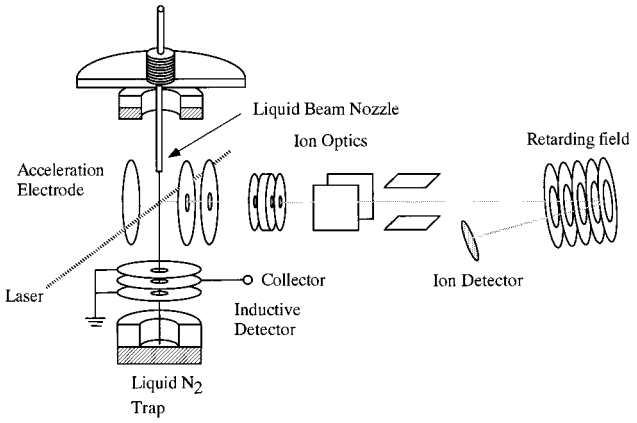

Figure 1. Schematic diagram of the liquid beam, the inductive detector, and the reflectron TOF mass spectrometer used in the present study. The liquid beam is crossed with a 266-nm laser 1 mm downstream from the nozzle. Photoions ejected from the liquid beam surface are mass analyzed by the TOF mass spectrometer, and those remaining inside the liquid beam are detected at 60 mm downstream from the ionization region by an inductive detector.

The effective pumping speed of the cryopump and another cryopump mounted in an upper part of the vacuum chamber (see Figure 1) was estimated to be 5000 L s^{-1}. The source chamber was evacuated additionally by a 1200 L s^{-1} diffusion pump, and the ambient pressure was typically $10^{-5}-10^{-6}$ Torr during injection of the liquid beam.

The liquid beam was crossed with a 266-nm fourth harmonic of a Quanta-ray GCR-11 Nd:YAG laser at 1 mm downstream from the nozzle in the first acceleration region of the TOF mass spectrometer. The laser was focused tightly into the liquid beam by sequentially aligned lenses with focal lengths of 250, −150, and 300 mm, and the diameter of the laser beam in the focusing point was 100 μm. The laser power was monitored by a LAS PM200 power meter. The tightly focused laser ionized molecules in the liquid beam. The ions thus produced are known to be partly ejected into vacuum with several accompanying molecules.[1] These ions in the gas phase were measured by the reflectron TOF mass spectrometer: The ejected ions were accelerated by a pulsed electric field in the first acceleration region in the direction perpendicular to both the liquid and the laser beams. The ions were then steered and focused by a set of vertical and horizontal deflectors and an einzel lens. The reflectron was provided with a reversing field tilted by 2° off the beam axis. After traveling a 0.5-m field-free region, a train of spatially separated ions was detected by a Murata EMS-6081B Ceratron electron multiplier. Signals from the multiplier were amplified and processed by a Yokogawa DL 1200E transient digitizer based on an NEC 9801 microcomputer. As the mass resolution, defined as $m/\Delta m$, depends strongly on the delay time from the laser photoionization to the pulsed acceleration for the mass spectrometry, the resolution was optimized by changing the delay time; the maximum resolution was attained to be 150 at the delay time of 1 μs. The dependency of the mass resolution originates from long duration of ions being ejected from the liquid beam.

The photoions remaining in the liquid beam as excess positive charges were detected 60 mm downstream from the ionization region by an inductive detector, which consists of three electrodes with a 10 mm aperture equidistantly separated by ceramic insulators 2 mm in thickness. In operation, the first and the third electrodes were grounded. The second electrode (collector) was directly connected to a Yokogawa DL1200E digital oscilloscope having an input impedance of 1.05 MΩ at 10 kHz, and the induction current was monitored. The flow velocity of the liquid beam was 16 ms^{-1} at the flow rate of 0.3 mL/min, so that the positively charged region generated by the photoionization in the liquid beam should pass through the detector 3.8 ms after the laser irradiation. The charge, q, induced in the collector electrode increases and then decreases as the charged region travels toward and away from the collector. In other word, the induction current into the collector increases at first, decreases, and then increases again with time: The induction current, i, is given by

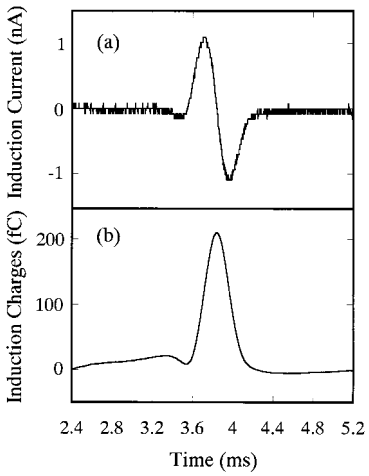

Figure 2. Time evolutions of a current (a) and a charge (b) at a collector induced by ions inside the liquid beam. The ions were produced by laser irradiation at 266 nm onto a liquid beam of a 0.2 M aniline solution in 1-propanol.

$$i = -\mathrm{d}q/\mathrm{d}t \qquad (1)$$

Results

Figure 2a shows the time evolution of the induction current detected at the collector; the induction current originates from the ions produced by irradiation of a 266-nm laser on the liquid beam of a 0.2 M aniline solution in 1-propanol. The origin of the time axis is set to be the time at which the 266-nm laser irradiates the liquid beam. Nearly antisymmetric peaks are observed; the positive peak arises from induction by the ions passing through the first and the second electrodes and the negative peak from induction by those passing through the second and the third electrodes. Figure 2b shows a time evolution of the induction charge obtained by integrating the induction current given in Figure 2a. The induction charge reaches the maximum at 3.85 ms, when the ions in the liquid beam flow through the collector. The arrival time of an ionized region at the collector agrees approximately with that calculated from the flow rate of the liquid beam of 20 μm diameter, when the flow rate is less than 0.2 mL/min. However, the measured arrival time tends to deviate from the calculated one as the flow rate exceeds this value, probably because of a slight expansion of the liquid beam on its injection from the nozzle. The diameter seems to increase almost linearly with the flow rate: 20.6 μm at 0.2 mL/min and 22.6 μm at 0.6 mL/min. The peak width agrees with that calculated from the transit time of the ionized region traveling through the collector. The agreement indicates that a diffusion length of the ions in the liquid beam along the liquid beam axis is much smaller than the dimension of the collector.

Figure 3 shows a mass spectrum of ions ejected into the gas phase after photoionization under the identical condition to those given in Figure 2. An aniline ion, AN^+, solvated with propanol

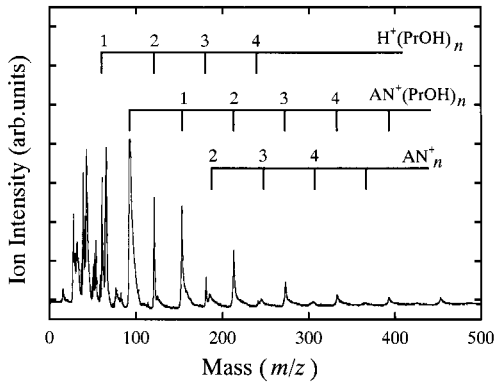

Figure 3. Mass spectrum of ions produced from a liquid beam of a 0.2 M aniline solution in 1-propanol by irradiation of a 266-nm laser. An aniline ion, AN^+, solvated with propanol molecules ($AN^+(PrOH)_n$ ($n = 1-6$)), protonated propanol cluster ions ($H^+(PrOH)_n$ ($n = 1-4$)), and aniline cluster ions (AN^+_n ($n = 1-5$)) are observed.

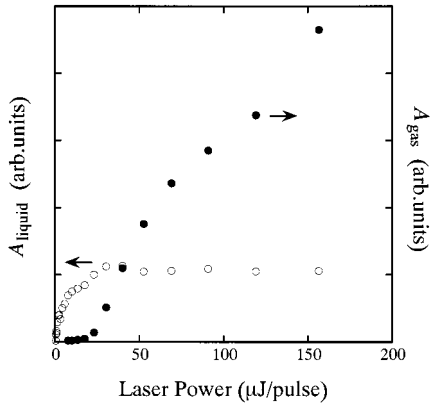

Figure 4. Abundance of ions inside the liquid beam, A_{liquid} (solid circle), and that of the cluster ions ejected into vacuum, A_{gas} (open circle) as a function of the laser power by the irradiation of the laser onto the 0.2 M aniline solution in 1-propanol.

molecules ($AN^+(PrOH)_n$ ($n = 1-6$)), protonated propanol cluster ions (H^+ $(PrOH)_n$ ($n = 1-4$)), and aniline cluster ions (AN^+_n ($n = 1-5$)), is observed in the mass spectrum. A part of the aniline ion and its fragment ions appearing at $m/z < 80$ are considered to be produced by ionization of aniline molecules in the gas phase evaporating from the liquid beam, because these ionic species were observed even when the ionization laser irradiates outside the liquid beam. On the other hand, the cluster ions are considered to be ejected from the liquid beam because these cluster ions were observed only when the laser beam irradiated the liquid beam.

Figure 4 shows the abundance of the ions (A_{liquid}) produced inside the liquid beam by laser irradiation onto the 0.2 M aniline solution in 1-propanol and that of the cluster ions (A_{gas}) ejected into the gas phase, as a function of the laser power.[20] As the laser power increases, A_{liquid} increases rapidly and then levels off at a laser power of ~25 μJ/pulse. On the other hand, A_{gas} rises at 25 μJ/pulse and gradually increases with the laser power. Even though the ions are generated inside the liquid beam by laser irradiation, no cluster ions in the gas phase are observed until the laser power exceeds a threshold value, 25 μJ/pulse.

A similar experiment was performed for pure liquid ethanol. Under irradiation of a 266-nm laser on the liquid beam of ethanol, the dominant cluster ion was $H^+(EtOH)_n$. The abundance of the ions (A_{liquid}) remaining inside the liquid beam and that of the cluster ion (A_{gas}) ejected into the gas phase were measured at different laser powers (see Figure 5).[21] As shown in Figure 5, A_{gas} starts to rise at a laser power of 40 μJ/pulse

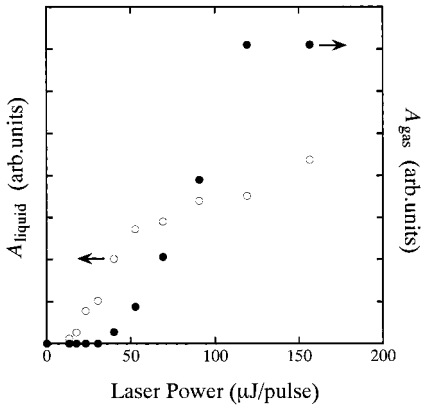

Figure 5. Abundance of ions inside the liquid beam, A_{liquid} (solid circle), and that of the cluster ions ejected into vacuum, A_{gas} (open circle), as a function of the laser power by the irradiation of the laser onto the pure ethanol liquid.

and increases with increase in the laser power; there exists a threshold laser power, below which no ion is ejected from the liquid beam surface. On the other hand, A_{liquid} increases rapidly, and then slowly above the threshold value of 40 μJ/pulse as the laser power increases.

Discussion

Photoionization of Aniline. An aniline solution in 1-propanol has a broad absorption band in a 284-nm region assigned to the S_0-S_1 transition of a solute aniline molecule and hence is excited into S_1 state by irradiation of a 266-nm laser.[22-25] The ionization potential of an aniline molecule on the solution surface was measured to be 6.4 eV.[26] It follows that if the solute molecule absorbs two photons simultaneously ($2h\nu = 9.32$ eV at 266 nm), the solute could be excited into the ionization continuum.[26] From a viewpoint of the energetics, an aniline solute molecule in S_1 state is ionized by absorbing one more photon. Resonant two photon ionization of liquid 1-propanol does not occur by irradiation of the 266-nm laser, because its absorption band in a 183-nm region is not reached resonantly by the 266-nm laser. It is concluded that aniline molecules in the solution are ionized almost exclusively by irradiation of the 266 nm laser. On the other hand, the formation of $H^+(PrOH)_n$ is ascribed to proton tranfer from AN^+ to a propanol molecule, because the abundance of $H^+(PrOH)_n$ changes similarly to that of $AN^+(PrOH)_n$.[15] The other formation via nonresonant photoionization of 1-propanol cannot be the dominant process because the abundance of $H^+(PrOH)_n$ decreases with the aniline concentration.

The electrons generated concurrently with the ionization in the solution are considered to have one of the following fates: (1) capture by a neutral molecule into a negative ion, (2) delocalize as solvated electrons, (3) geminate recombination with cations, and (4) liberate as free electrons in the gas phase. The free electron liberation (case 4) takes place particularly in the vicinity of the surface, so that a surface region with a depth of several nanometers at most turns out to be positively charged due to electron depletion from the surface region. When a repulsive Coulomb energy exerted to an ion of interest from its neighboring ions exceeds the solvation energy of the ion, the ion is ejected from the surface (Coulomb ejection model).

As described above, aniline ions are dominantly produced in the aniline solution of 1-propanol. Suppose that an aniline ion, AN^+, is about to leave the solution surface by the Coulomb repulsion built by its neighboring aniline ions, AN^+ attracts its surrounding solvent molecules and is ejected with several

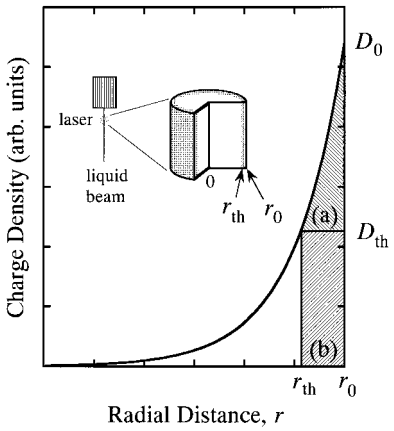

Figure 6. Charge density distribution with respect to the radial direction. The charge density decreases exponentially from the liquid surface. The ions in the hatched portion (a) and the portions (a) + (b) are supposed to be ejected into vacuum in cases I and II, respectively.

accompanying 1-propanol molecules, PrOH, as $AN^+(PrOH)_n$ in the gas phase.[15] The nascent cluster ion, $AN^+(PrOH)_n$, undergoes unimolecular dissociation in the gas phase before it is detected as $AN^+(PrOH)_m$. Similarly, the detection of AN^+_n indicates that several aniline molecules aggregate on the surface and are ejected together with AN^+. The presence of protonated propanol cluster ions in the mass spectrum implies that protons are produced in the course of the aniline ionization.

Ion Ejection Mechanism. Let us consider that the solute molecules are dissolved homogeneously in a cylindrical liquid beam with a radius r_0 and density $D(r)$ of excess positive charges resulting from the photoionization, and subsequent electron liberation in the vicinity of the surface is supposed to decrease exponentially with the depth from the liquid surface, $r_0 - r$. The density, $D(r)$, is expressed as

$$\mathrm{D}(r) = D_0 \exp(-(r_0 - r)/R) \tag{2}$$

where r is a radial distance from the center of the liquid beam, D_0 is a density of the ions on the liquid surface, R is an escape depth of the electron produced concurrently with ion formation (see Figure 6). The exponential decrease of $D(r)$ with $r_0 - r$ is consistent with the fact that the escape probability of an electron decreases exponentially with the depth. In the Coulomb ejection model, ions on the surface are assumed to be ejected out of the liquid beam from a region where $D(r)$ exceeds the threshold ion density, D_{th}.

The excess ions on the outermost layer of the solution surface are liberated into vacuum, because they are repelled by the ions neighboring the outermost layer toward the surface by the Coulomb repulsive force. If the ions diffuse to the surface much faster than the ions are liberated into the vacuum, the surface is always filled with the ions supplied from the inside. As a result, the portion of the ions whose density is larger than D_{th} are ejected into the vacuum and otherwise remain in the liquid beam (case I). In contrast, if the ion diffuses at a comparable or slower rate than the ion ejection, the ions on the outermost layer of the solution surface are sequentially ejected from the surface. In this case, all the ions in $r > r_{th}$ are ejected from it, and the ions which exist in $r < r_{th}$ are left inside the liquid beam (case II), where $D_{th} = D(r_{th})$. The laser-power dependence of the ion intensity in the case of pure ethanol is well explained in the framework given by case I, where a proton generated in the ethanol diffuses at a rate (9.3×10^{-9} m^2 s^{-1}), 1 order of magnitude larger than those of typical ionic species ($(1-2) \times 10^{-9}$ m^2 s^{-1}).[28-30] Note that much faster proton transfer is conceivable, such as a long-range proton jump. Therefore, the ion supply toward the surface must be complete before the ion ejection. On the other hand, the aniline solution in 1-propanol falls into case II because the aniline ion, which is the main charge carrier, diffuses at a slow rate so that the rate-determining step is the ion supply toward the surface. The presence of protonated propanol cluster ions in the mass spectrum implies that protons are produced in the course of the aniline ionization. However, case II is operative because the rate-determining process involves the aniline ion having a small diffusion rate.

Coulomb Ejection Model. As mentioned above, two cases are conceivable in the ion ejection process: Only the excess ions whose density are larger than D_{th} are ejected into vacuum and otherwise they remain in the liquid beam (case I), or all the charges in $r > r_{th}$ are ejected from the surface (case II). As illustrated in Figure 6, the ions in the hatched portion a and the portions a + b are considered to be ejected into vacuum in cases I and II, respectively. A total number of ions remaining inside the liquid beam, N_{liquid}, and that ejected into the vacuum, N_{gas}, calculated by integrating the number of the ions in a region which meets with the condition of case I or case II is given, respectively, as follows: In case I

$$N_{liquid} = \int_0^{r_0} 2\pi hrD(r)\,\mathrm{d}r \qquad \text{for} \quad D_0 < D_{th} \tag{3}$$

$$N_{liquid} = \int_0^{r_{th}} 2\pi hrD(r)\,\mathrm{d}r + \int_{r_{th}}^{r_0} 2\,\pi hr\,D(r) \qquad \text{for} \quad D_0 > D_{th} \tag{4}$$

$$N_{gas} = \int_{r_{th}}^{r_0} 2\pi hr(D(r) - D_{th})\,\mathrm{d}r \quad \text{for} \quad D_0 > D_{th} \tag{5}$$

and in case II

$$N_{liquid} = \int_0^{r_0} 2\pi hrD(r)\,\mathrm{d}r \qquad \text{for} \quad D_0 < D_{th} \tag{6}$$

$$N_{liquid} = \int_0^{r_{th}} 2\pi hrD(r)\,\mathrm{d}r \qquad \text{for} \quad D_0 > D_{th} \tag{7}$$

$$N_{gas} = \int_{r_{th}}^{r_0} 2\pi hrD(r)\,\mathrm{d}r \qquad \text{for} \quad D_0 > D_{th} \tag{8}$$

where h is the height of the ionization region along the liquid beam. As R/r_0 is negligibly small ($R \sim 1$ nm, $r_0 \sim 10$ μm), eqs 3−8 are simplified as follows: In case I

$$N_{liquid} = SD_0 \qquad \text{for} \quad D_0 < D_{th} \tag{9}$$

$$N_{liquid} = S(D_{th} - D_{th}\ln(D_{th}/D_0)) \qquad \text{for} \quad D_0 > D_{th} \tag{10}$$

$$N_{gas} = S(D_0 - D_{th} + D_{th}\ln(D_{th}/D_0)) \qquad \text{for} \quad D_0 > D_{th} \tag{11}$$

and in case II

$$N_{liquid} = SD_0 \qquad \text{for} \quad D_0 < D_{th} \tag{12}$$

$$N_{liquid} = SD_{th} \qquad \text{for} \quad D_0 > D_{th} \tag{13}$$

$$N_{gas} = S(D_0 - D_{th}) \qquad \text{for} \quad D_0 > D_{th} \tag{14}$$

where S ($= 2\pi r_0 Rh$) is the volume of the ion ejection region. In other words, the surface of the cylindrical liquid beam can be treated as if it were a flat surface having an equivalent surface area to that of the liquid beam. The charge density, D_0, on the surface is related to the laser power, I, as

$$D_0 = kCI^n \tag{15}$$

where C represents the solute concentration, n is a number of

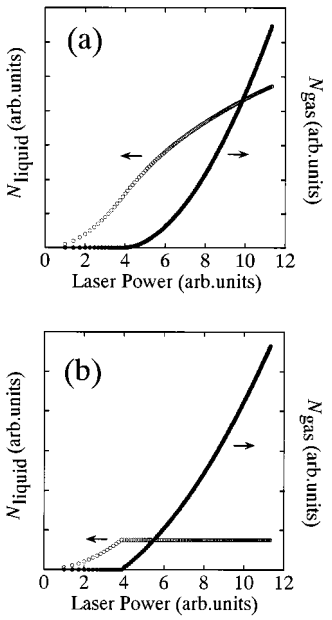

Figure 7. Number of ions produced inside the liquid, N_{liquid}, and in the gas phase, N_{gas}, as a function of the laser power, I, is shown schematically for $n = 2$. The gas-phase ion abundance starts to rise at a threshold laser power, I_{th}, and rapidly increases in both cases. On the other hand, N_{liquid} increases with the laser power and then becomes saturated at I_{th} for case I (a), and it completely levels off at I_{th} for case II (b).

photons involved in the ionization, and k is a coefficient independent of C, I, and n. The dependences of N_{liquid} and N_{gas} on the laser power, I, are calculated and shown in Figure 7 for $n = 2$. The number of the ions in the gas phase (N_{gas}) starts to rise at a threshold laser power, I_{th}, and increases as the laser power increases for both cases I and II. On the other hand, N_{liquid} increases with the laser power and then tends to increase slowly above I_{th} in case I, while it becomes almost constant above I_{th} in case II. In the ionization of pure ethanol, the laser-power dependence of A_{liquid} is reproduced well in the framework of case I (see Figure 5), while in an aniline solution in 1-propanol, case II is valid (see Figure 4).

In this model, we disregard the time dependence of the radial distribution of the excess ions and that of the ion ejection: In reality, the ions are liberated from the surface more rapidly at the beginning of the ion ejection than in the latter process, since the rate for the ion ejection depends on the density of the excess ions in the liquid beam. The neglect of such effects does not seem to introduce serious defects into the model.

Characterization of Liquid Beam. Figure 8 shows A_{liquid} and A_{gas}, which were measured under irradiation of the 266-nm laser onto the liquid beam of pure ethanol with changing the distance between the laser beam and the liquid beam. The ion intensity, A_{liquid}, is found to be zero within the experimental uncertainty, when the two beams do not overlap each other. In a position where the laser beam overlaps with the liquid beam, A_{liquid} depends on the geometry of the interaction region of the liquid beam (20 μm in diameter) with the laser beam (100 μm in diameter): The photon density of the laser beam is the highest at the beam center and shows a Gaussian-like decrease with the distance from the center. Considering that ethanol molecules are ionized by nonresonant two-photon absorption and the ionization probability is proportional to the square of the laser power, a Gaussian-like laser beam profile is manifested approximately in a plot of the square root of A_{liquid} as a function of the position of the laser (see the inset of Figure 8).[31]

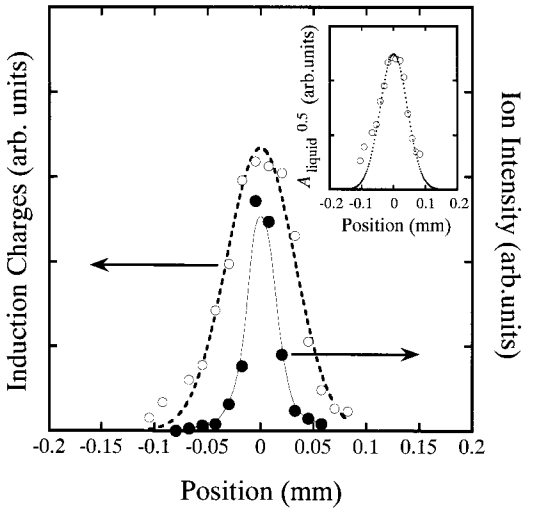

Figure 8. Abundance of ions in the liquid beam, A_{liquid} (open circle), and that of ions in the gas phase, A_{gas} (solid circle), produced by irradiation of the 266-nm laser onto the liquid beam of the pure ethanol liquid, as a function of the distance between the laser beam and the liquid beam. As shown in the inset, a Gaussian-like laser beam profile is manifested approximately in a plot of the square root of A_{liquid}.[30]

On the other hand, A_{gas} is intense only when the beam center of the laser crosses with the liquid beam, while no ions are produced in the gas phase even when the laser beam grazes the liquid beam; A_{gas} also depends sensitively on the geometry of the interaction region of the two beams, and ions are ejected from the surface when the photon density at the interaction region exceeds the threshold.

The dependences of A_{gas} and A_{liquid} on the distance between the laser beam and the liquid beam show that formation of ions in the gas phase always involves formation of ions inside the liquid; no cluster ions are produced in the gas phase unless the laser ionizes the molecules inside the liquid beam. Our previous studies show that the cluster ions are produced from the liquid beam, as the cluster ions are observed only when the laser beam irradiates the liquid beam. Note that the diameter of the laser beam is much larger than that of the liquid beam. The present results also support the previous one, because the ions remaining inside the liquid beam provide information on the geometry of the interaction region of the liquid beam with the laser beam. These facts lead us to conclude that the boundary region between the liquid beam surface and the gas phase is clear-cut, and no clusters exist over the liquid beam surface.

Conclusion

The ion ejection mechanism from the liquid beam surface following laser multiphoton ionization was examined by observing simultaneously ions ejected from the liquid surface and those remaining inside the liquid beam. The laser-power dependence of the ion intensities of interest is explained principally in the framework of a Coulomb ejection scheme. An amount of ions ejected from the surface differs by the diffusion rate of the ions.

Acknowledgment. We are grateful to Dr. Thomas Leisner of Freie Universität Berlin for useful suggestions and Mr. Yoshihiro Takeda for his assistance in the early stage of the liquid beam studies. This work was supported by the Special Cluster Research Project of the Genesis Research Institute, Inc.

References and Notes

(1) Mafuné, F.; Takeda, Y.; Nagata, T.; Kondow, T. *Chem. Phys. Lett.* **1992**, *199*, 615.

(2) Mafuné, F.; Kohno, J.; Nagata, T.; Kondow, T. *Chem. Phys. Lett*. **1994**, *218*, 7.
(3) Faubel, M.; Schlemmer, S.; Toennies, J. P. *Z. Phys. D* **1988**, *10*, 269.
(4) Faubel, M.; Kisters, Th. *Nature* **1989**, *339*, 527.
(5) Faubel M.; Steiner B.; Toennies, J. P. *Mol. Phys.* **1996**, *90*, 327.
(6) Faubel M.; Steiner B.; Toennies, J. P. *J. Chem. Phys.* **1997**, *106*, 9013.
(7) Mafuné, F.; Kohno, J.; Nagata, T.; Kondow, T. *Chem. Phys. Lett.* **1994**, *218*, 234.
(8) Mafuné, F.; Hashimoto, Y.; Hashimoto, M.; Kondow, T. *J. Phys. Chem.* **1995**, *99*, 13814.
(9) Kohno, J.; Mafuné, F.; Kondow, T. *J. Am. Chem. Soc.* **1994**, *116*, 9801.
(10) Horimoto, N.; Mafuné, F.; Kondow, T. *J. Phys. Chem.* **1996**, *100*, 10046.
(11) Matsumura, H.; Mafuné, F.; Kondow, T. *J. Phys. Chem.* **1995**, *99*, 5861.
(12) Holstein, W. L.; Hayes, L. J.; Robinson E. M. C.; Laurence, G. S.; Buntine, M. A. *J. Phys. Chem.* B **1999**, *103*, 3035.
(13) Kleinkofort, W.; Pfenninger, A.; Plomer, T. Griesinger, C.; Brutschy, B. *Int. J. Mass Spectrom. Ion Proc.* **1996**, *156*, 195.
(14) Sobott, F.; Kleinekofort, W.; Brutschy, B. *Anal. Chem.* **1997**, *69*, 3587.
(15) Mafuné, F.; Kohno, J.; Kondow, T. *J. Chin. Chem. Soc.* **1995**, *42*, 449.
(16) Morgner, H. In *Linking the Gaseous and Condensed Phases of Matter*, Christophorou, L. G., Illenberger, E., Schmidt, W. F., Eds.; Plenum Press: New York, 1994.
(17) Krämer, B.; Hübner, O.; Heβ, H.; Leisner, T. *Euro. Phys. J. D*, in press.
(18) In the aniline/1-propanol solution, the ion intensity in the gas phase increases quadrically with the laser power.[15] It implies that the ion ejection involves two photons and no more photons are needed. It follows, therefore, that laser stimulated emission, Coulomb explosion of divalent ions, Auger processes, etc. should be ruled out from the consideration because they require more than two photons.
(19) Horimoto, N.; Mafuné, F.; Kondow, T. *J. Phys. Chem*. Submitted.
(20) The abundance of the cluster ions in the gas phase, A_{gas}, is given by $A_{gas} = \sum_{n=1}[AN^+(PrOH)_n] + \sum_{n=1}[H^+(PrOH)_n] + \sum_{n=2}[AN^+{}_n]$ where [ ] represents the abundance of each cluster ion.
(21) The abundance of the cluster ions in the gas phase, A_{gas}, is given by $A_{gas} = \sum[H^+(PrOH)_n]$ where [ ] represents the abundance of each cluster ion.
(22) Absorption spectrum of aniline in *n*-propanol was observed by using a Shimadzu UV-1200 spectrometer.
(23) Jacon, M.; Lardeux, C.; Lopez-Delgado, R.; Tramer, A. *Chem. Phys.* **1977**, *24*, 145.
(24) Kohler, G. *J. Photochem.* **1987**, *38*, 217.
(25) Horimoto, N.; Mafuné, F.; Kondow, T. *J. Phys. Chem*. In press.
(26) Horimoto, N.; Mafuné, F.; Kondow, T. In preparation.
(27) In *CRC Handbook of Chemistry and Physics*, 78th ed.; Lide, D. R., Ed.; CRC Press: New York, 1997.
(28) Debye, P.; Trans. *Electrochem. Soc.* **1942**, *82*, 265.
(29) Umberger, J. Q,; La Mer, V. K. *J. Am. Chem. Soc*. **1945**, *67*, 1099.
(30) Eigen M.; Eyring, E. M. *J. Am. Chem. Soc.* **1962**, *84*, 3254.
(31) As the diameter of the laser beam in the ionization region is larger than that of the liquid beam, the number of photons interacting with the liquid beam depends on the geometry of the two beams. The normalized two-dimensional photon-density distribution, $F(x, y)$, is given by, $F(x, y) = (4 \ln 2)/(a^2\pi) \exp([-4 \ln 2 (x^2 + y^2)]/a^2)$, where x and y are the axes orthogonal to the laser beam axis and a is the diameter at the half-maximum intensity of the laser beam. The number of photons interacting with the liquid beam, $P(d)$, is then given by $P(d) = \int_{d-w/2}^{d+w/2} dx \int_{-\infty}^{\infty} dy\, F(x, y) = [(4 \ln 2)]^{1/2}/(a\pi^{1/2}) \int_{d-w/2}^{d+w/2} \exp((-4 \ln 2\, x^2)/a^2)\, dx$, where d and w represent the distance between the laser beam center and the liquid beam and the diameter of the liquid beam, respectively. Practically, the integral in the equation above cannot be dissolved analytically but is calculated numerically using a error function as $P(d) = [(4 \ln 2)^{1/2}]/(a\pi^{1/2})(\int_{-\infty}^{d+w/2} \exp((-4 \ln 2\, x^2)/a^2)\, dx - \int_{-\infty}^{d-w/2} \exp((-4 \ln 2\, x^2)/a^2))\, dx$. The line in the inset of Figure 8 shows the fitting of the equation above for $a = 100\ \mu$m and $w = 20\ \mu$m and reproduces well the experimental result.